



ELSEVIER

Contents lists available at ScienceDirect

Opto-Electronics Review

journal homepage: <http://www.journals.elsevier.com/opto-electronics-review>

Electronic and optical properties of vacancy and B, N, O and F doped graphene: DFT study

M. Goudarzi^a, S.S. Parhizgar^{a,*}, J. Beheshtian^b

^a Plasma Physics Center, Science and Research Branch, Islamic Azad University, Tehran, Iran

^b Institute for Advanced Technologies, Shahid Rajaee Teacher Training University, 16875-163, Lavizan, Tehran, Iran

ARTICLE INFO

Article history:

Received 6 September 2018

Received in revised form 12 April 2019

Accepted 6 May 2019

Available online 24 May 2019

Keywords:

Graphene

Density functional theory

Structural and optical properties

Absorption spectra

ABSTRACT

Structural and optical properties of graphene with a vacancy and B, N, O and F doped graphene have been investigated computationally using density functional theory (DFT). We find that B is a p-type while N, O and F doped graphene layers, as well as graphene with a vacancy are n-type semiconductors. Optical properties for both cases of in plane ($E \perp c$) and out of plane ($E \parallel c$) polarization of light are investigated. It is observed that with the increase in the number of electrons entering the supercell, the amount of absorption of the system decreases and the absorption peaks are transferred to higher energies (blue shift).

© 2019 Association of Polish Electrical Engineers (SEP). Published by Elsevier B.V. All rights reserved.

Introduction

Since the discovery of the single layer of graphite, which is called graphene [1], this two dimensional layers, graphene-based and other 2D materials have been extensively investigated for more electronic, magnetic and optical applications theoretically [2–4] and experimentally [5–8]. These potential applications continue the extent from the photovoltaic cell and ultracapacitors to spin-transport electronics [9–12]. Graphene also has many unique physical properties, these include a band gap of zero at the so-called Dirac point, a dispersion relation equivalent to that of massless Dirac fermions near the Dirac point and low spin-orbit coupling. Optical properties of graphene are anisotropic with respect to the light polarization being parallel or perpendicular to the normal to the layer [13].

Graphene doping with impurities or atom adsorption on graphene further influences its conductive, optical and magnetic properties [14,15]. For example, adsorbing an H atom by graphene leads to significant magnetic moment while pure graphene is non-magnetic [16]. Adatoms also influence the electronic properties of graphene [17], by shifting the energy of the Dirac point, changing the density of states (DOS) near the point and altering electron and hole mobilities [14].

A great amount of effort has been devoted to open a tunable band gap in graphene. According research by P.A. Denis [18], doping graphene with Al, converts its structure into metal while doping with Si, P and S atoms causes band gap opening dependent on the concentration of the doped atom. In the work of M. Rafique *et al.* [19] they investigated the effect of a 3d metal trioxide clusters-doped monolayer graphene on structural electronic and magnetic properties. Also M.S. Sharif Azadeh *et al.* [20] showed that by inserting Si into graphene, a band gap is created and its magnitude increases with increasing the density of impurities.

In this work, we investigate the structural properties of doping graphene with atoms in the row of carbon atom in the periodic table (B, N, O and F) and graphene with a vacancy. With this type of doping we study the effect of the change in the number of electrons on the structures. In this research we have used density functional theory (DFT) method that, the exchange-correlation term, was employed in GGA approximation. Furthermore, changes in electronic and optical properties caused by doped in graphene layer will be discussed. Optical properties of pure graphene have been investigated by many researchers. e. g. Y.H. Ho *et al.* [21] but these properties are rarely considered for doped graphene, therefore, in part of this study, we examine the optical properties of the structures in question.

It should be noted that M. Wu *et al.* [22] have calculated the effect of graphene doping with B, N, O and F atoms with 2% impurities concentration and they used VASP software. In the calculation that was performed by them, the optical effect has not been investigated while we study both electronic and optical properties with

* Corresponding author at: Plasma Physics Center, Science and Research Branch, Islamic Azad University, Tehran, Iran.

E-mail address: ssparhizgar@gmail.com (S.S. Parhizgar).

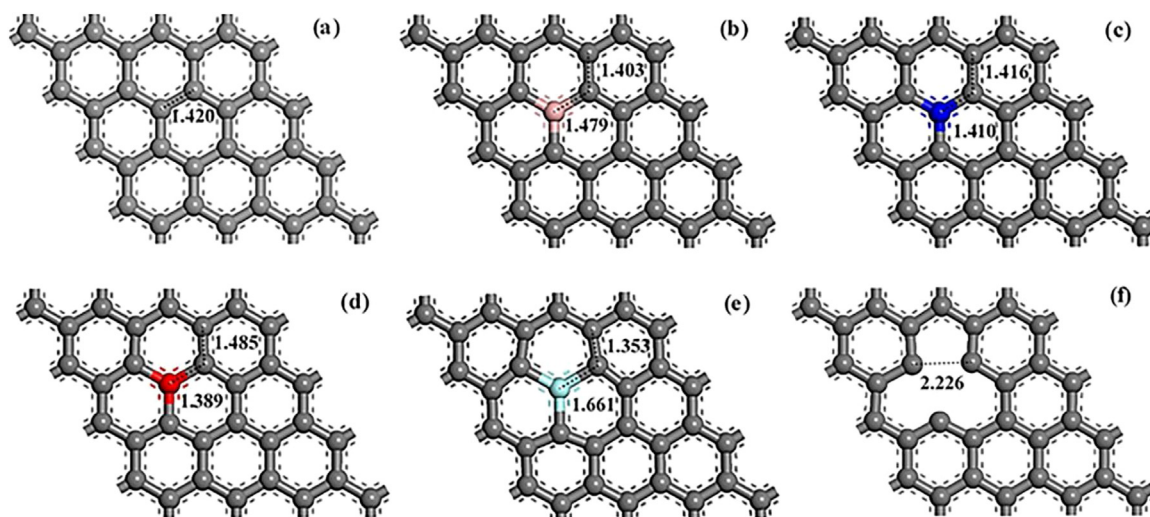


Fig. 1. Optimized supercell 4×4 with 32 atoms for (a) pure graphene, (b) B doped graphene, (c) N doped graphene, (d) O doped graphene, (e) F doped graphene and (f) graphene with a vacancy.

the 3.125% impurities concentration and by Quantum espresso code.

Methods

In this work, all calculations were performed by a spin-polarized DFT implemented in a Quantum Espresso code [23], which is based on the plane-wave pseudopotential method.

In this model, the $4 \times 4 \times 1$ graphene supercell that contains 32 carbon atoms has been used. For this supercell, lattice parameters are $a = b = 9.84 \text{ \AA}$, $\gamma = 120^\circ$ and C–C bond length is 1.42 \AA , and in order to ensure that there is no interaction between graphene sheets, vacuum slab of 15 \AA is adopted. In this model of calculation, a plane-wave basis set with a maximum plane-wave energy of 340 eV cutoff is used in combination with ultrasoft potential. The generalized gradient approximation (GGA), proposed by Perdew–Burke–Ernzerhof (PBE), is used to deal with the Exchange–Correlation term [24]. All systems were optimized through fully relaxing the atomic structures until the remaining force were smaller than 0.01 eV/\AA . The occupation state is smearing and the value of Gaussian spreading for Brillouin-zone integration is 0.01 eV , and the maximum spacing between K points was 0.03 \AA^{-1} .

This work has two parts: first electronic structural for doped graphene with B, N, O, and F atoms and graphene with a vacancy are studied and, then the effect of these atoms and a vacancy on optical properties of graphene are investigated. Band structure, electron density of states and optical properties have been calculated for the symmetric path of $\Gamma\text{K}\text{M}\Gamma$ in Brillouin-zone.

In our work, electronic and optical properties of doped graphene with atoms in the second row in the periodic table corresponding to the p group ($2p^1$, $2p^3$, $2p^4$ and $2p^5$) and graphene with a vacancy are calculated. In this way, we obtain the effect of increasing the number of electrons imported in the supercell on the type of bonds, bonds length and structural and optical properties.

Results and discussions

Electronic properties are calculated and maximum valence band (MVB) and Fermi level are set to zero.

In all cases, the graphene with a vacancy and doped graphenes remain planar so that new structures like pure graphene have sp^2 hybridization, these planar structures have been confirmed

by Wang *et al.* experimental work recently [25]. The optimized supercell model of each structure is shown in Figs. 1(a)–(f). After geometry optimization, maximum and minimum X–C bond lengths (d_{xc}) belong to F and N atoms, respectively and are equal to 1.661 \AA and 1.410 \AA . For N atom doped graphene this length is consistent with other experimental work. In confirming our theoretical work, Z. Xing *et al.* showed in an experimental research that N–C bond length is 1.41 \AA and this result is in full agreement with our work [26]. For neither of structures except graphene with a vacancy and F doped graphene, there is no difference for up and down electron spin on the band structure, so these structures are non-magnetic. Band gaps, magnetic moments and X–C and C–C average bond lengths for any structure are given in Table 1.

Electronic properties

The band structure diagrams for all doped graphene structures and graphene with a vacancy are presented in Figs. 2(b)–(f). Band structure diagram of pure graphene is also shown in Fig. 2(a) in order to determine the effect of the atom-doping on the electronic structure of graphene. Figure 2(a) shows pure graphene has zero band gap in Dirac point; in this point, the valence band (π) and conduction band (π^*) straddling each other at Fermi level which is consistent with other literatures [27,28].

As it can be seen from Figs. 2(b)–(e), doping graphene layers with different atoms have a large effect in graphene band structures. The most notable feature is represented by the change in the electronic properties, and in particular by the possibility to induce small energy band gap and p-type or n-type conductivity.

In this work it was found that 3.125% boron doped graphene indicates a p-type conductivity which is in consistent with S. Agnoli *et al.* experimental results [29] and M. Wu *et al.* theoretical research [22]. Due to the dopant, the graphene slightly distorts, such that the B–C bond is 1.479 \AA . It is also observed that substitution boron atom in $4 \times 4 \times 1$ graphene layer causes the Fermi level shifts down about 0.874 eV with respect to the Dirac energy while this shift for $5 \times 5 \times 1$ supercell in M. Wu *et al.* work is 0.7 eV and B–C bond length is 1.49 \AA . The doped boron atom causes a band gap approximately 0.186 eV at high symmetric K-point as shown in Fig. 2(b) and exhibits metallic behavior as some surface states are present at Fermi level and in M. Wu *et al.* work gap is 0.14 eV that disagreements are due to differences in the doped atomic ratio of the graphene layer.

Table 1
Band gap, Magnetic moment, d_{C-C} average bond length of carbons and d_{X-C} indicates bond length of doped and carbon atoms for pure graphene, graphene with a vacancy and doped graphene.

System	Pure graphene	Graphene with a vacancy	B doped graphene	N doped graphene	O doped graphene	F doped graphene
Band gap (eV)	0.000	---	0.186	0.203	0.494	0.367 (up) 0.546 (down)
Magnetic moment (μ_B)	0.000	0.890	0.000	0.000	0.000	0.980
d_{C-C} (Å) (average)	1.420	1.400	1.403	1.416	1.389	1.353
d_{X-C} (Å)	--	--	1.479	1.410	1.485	1.661

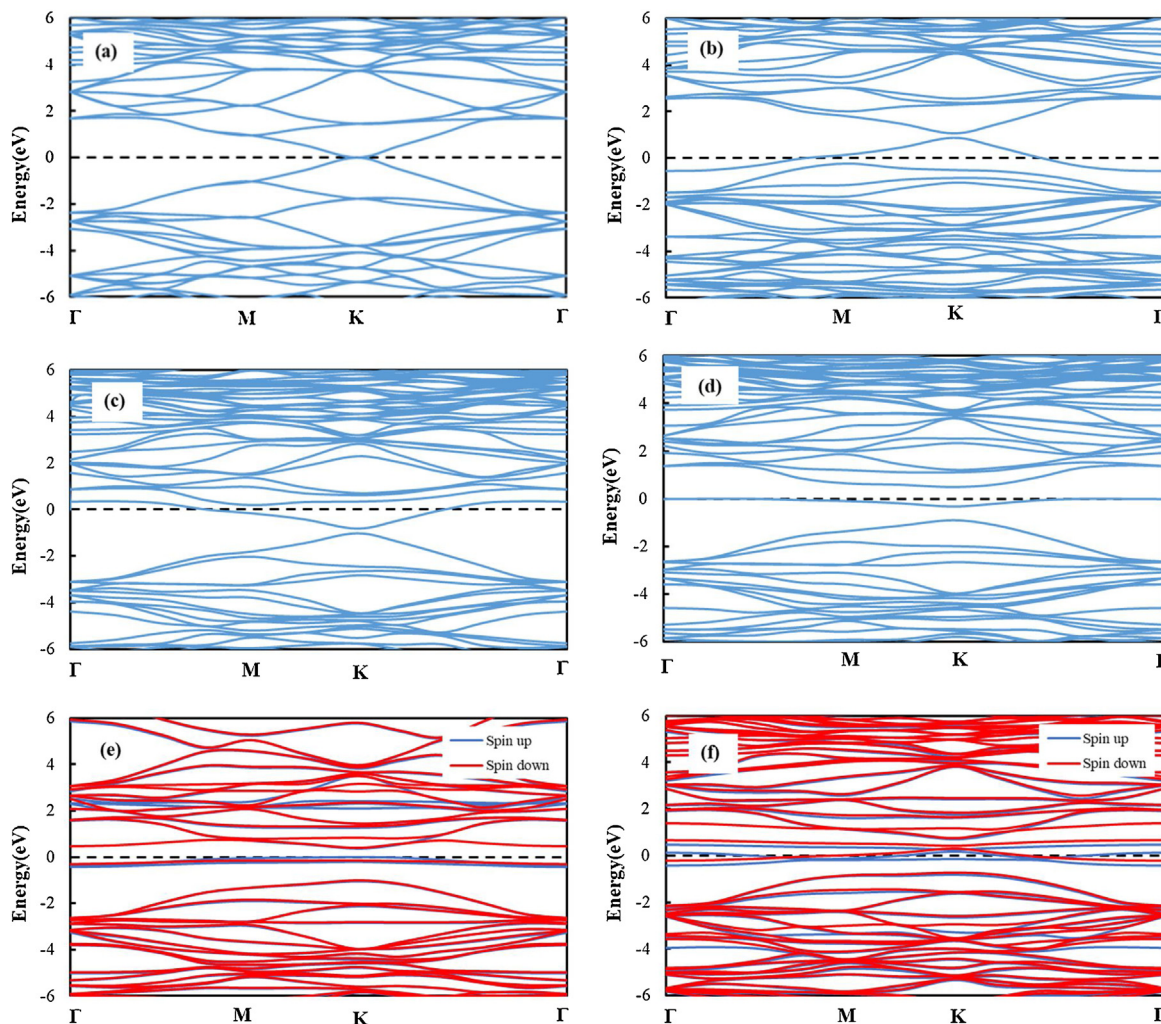


Fig. 2. Band structure of (a) pure graphene in the 4×4 supercell, (b) B doped graphene, (c) N doped graphene, (d) O doped graphene, (e) F doped graphene and (f) graphene with a vacancy.

If graphene layer doped with 3.125% N atom, N–C bond length is 1.41 Å and Fermi level is shifted up about 0.817 eV. This result indicates that the n-type semiconducting behavior of graphene is in agreement with the M. Wu *et al.* theoretical research [22] and experimental work of L. S. Panchakarla *et al.* [30], this result has also been confirmed by Wang *et al.* experimental work [25,31]. Like boron doped, the doped graphene with nitrogen atom has a band gap approximately 0.203 eV at high symmetric K-point as shown in Fig. 2(c) and displays metallic behavior as some surface states are present at Fermi level which is in agreement by other theoretical reports [32,33], that done by VASP while our work has been done with Quantum espresso. In M. Wu *et al.* calculation that the effect of graphene doping has been investigated with 2% impurities concentration, N–C bond length has been reported 1.42 Å, fermi level shift 0.7 eV and band gap 0.14 eV; furthermore, in M. Rafique *et al.* research [32] that most closely resembles our work, N–C bond

length has been mentioned about 1.408 Å, fermi level shift 0.8 eV and band gap 0.1526 eV.

Similar to N atom substitution, 3.125% O atom doped graphene also is a n-type semiconductor and displays indirect band gap about 0.494 eV as shown in Fig. 2(d) and the O–C bond length has been measured 1.485 Å, these results are comparable to M. Wu *et al.* results with 2% impurities concentration that showed O–C bond length is about 1.50 Å, and band gap is 0.5 eV [22]. In this case, we can find a flat band appears between the valence and conductive band which due to the O atom orbitals.

In case of the graphene layer doped with 3.125% F atom, like N and O doped graphene, the structure is an n-type semiconductor and has a direct band gap approximately about 0.367 eV and 0.546 eV for spin up and spin down cases, respectively as can be seen from Fig. 2(e), also F–C bond length in this structure is 1.661 Å. Two additional bands have been created between the valence band

and conduction band that arising from the presence of F atom in the graphene layer. This structure has a magnetic moment of $0.98 \mu_B/\text{cell}$ which is comparable to M. Wu *et al.* work [22], in their research, for doped one F atom in $5 \times 5 \times 1$ graphene supercell, the magnetic moment is $0.71 \mu_B/\text{cell}$ and in no other reference, there is no structural data for F doped graphene. Different energy gaps for up and down spin, makes this structure suitable for use in spintronic tools.

As can be seen in Fig. 1(f), the graphene with a vacancy undergoes a John-Teller distortion which leads to the saturation of two of the three dangling bonds toward the missing atom. One dangling bond always remains owing to geometrical reasons. This leads to the formation of a five-membered and a nine-membered ring [34]. It was found that band structures of graphene with a vacancy in the spin up and down cases are an n-type semiconductor and as shown in Fig. 2(f) has additional bands between the valence band and conduction band that cut the Fermi level, then this structure similar to B and N doped graphene has metallic behavior due to some states that present at Fermi level. Graphene with a vacancy has magnetic moment of $0.89 \mu_B/\text{cell}$ and two of the carbon atoms close to the vacancy site move towards each other forming a C–C distance of 2.226 \AA like other's report [22,28]. In M. Wu *et al.* results with 2% impurities concentration, the magnetic moment is measured about $1.58 \mu_B/\text{cell}$ and C–C bond length is 2.17 \AA .

Now consider what happens to the fermi level when the graphene layer is doped with the B, N, O and F atoms. One aspect of this process is the principle of electronegativity equalization consideration to predict what happens. Since the B atom is more electropositive than carbon atom [35], the bonding of this atom with its adjacent carbon atoms in the graphene layer causes the flowing of electrons from carbon atoms in graphene layer to B atom, then this structure turns into a p-type semiconductor. In this case the density of states below the band gap increases and according to the fermi equation, the fermi level in the graphene layer decreases. About the cases of N, O and F atoms, these are more electronegative than carbon atom [35]; consequently, by creating a bond between these atoms and carbon atoms in graphene layer, electrons have to flow from N, O and F atoms to carbon atoms, then these structures turn into an n-type semiconductor. In this case the density of states above the band gap increases and according to the fermi equation, the fermi level energy in the graphene layer increases, too [36,37].

Optical properties

We calculated optical properties produced electronic energies on the Monkhorst-Pack mesh of k-points and the matrix elements for electronic interband transitions, so there can be some inaccuracy in dielectric function results at low energies. In order to calculate the absorption coefficient, α , we need dielectric tensor values. Dielectric constant is the sum of real and imaginary part, i.e. $\varepsilon = \varepsilon_1 + i\varepsilon_2$ together. The imaginary part can be calculated by the summation of empty states using following equation:

$$\varepsilon_2(\mathbf{q} \rightarrow \mathbf{o}, h\omega) = \frac{2\pi e^2}{\Omega \varepsilon_0} \sum_{\mathbf{K}, \mathbf{K}', v, c} |\langle \psi_{\mathbf{K}'}^c | \mathbf{u} \cdot \mathbf{r} | \psi_{\mathbf{K}}^v \rangle|^2 \delta(E_{\mathbf{K}'}^c - E_{\mathbf{K}}^v - E). \quad (1)$$

Where the indices c and v refer to conduction and valence band, $\psi_{\mathbf{K}}^c$ and $\psi_{\mathbf{K}}^v$ are eigenfunctions with $E_{\mathbf{K}}^c$ and $E_{\mathbf{K}}^v$ eigenvalues, respectively.

The real part of dielectric tensor is obtained by using Kramers-Kronig transformation:

$$\varepsilon_1(\omega) = 1 + \frac{2}{\pi} P \int_0^{\infty} \frac{\varepsilon_2(\omega') \omega'}{\omega'^2 - \omega^2 + i\eta} d\omega'. \quad (2)$$

Where P denotes the principle value.

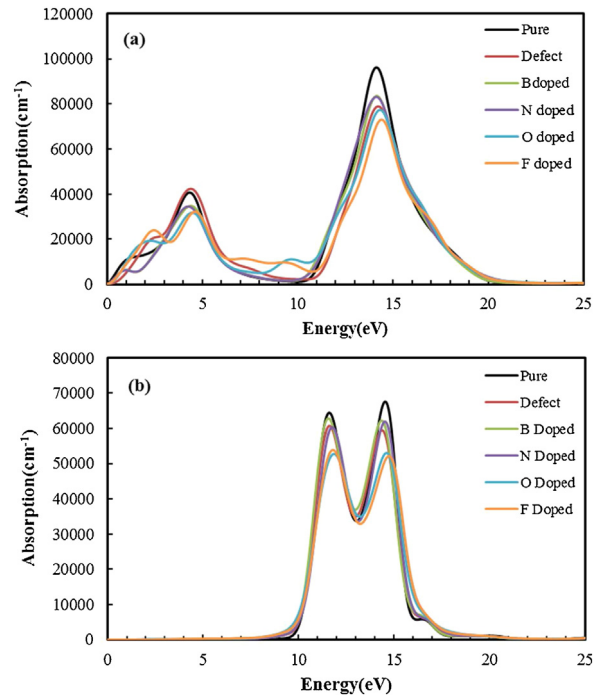


Fig. 3. Absorption coefficient (a) for in plane ($E \perp c$) and (b) out of plane ($E \parallel c$) polarization of light.

After getting dielectric tensor values, we can easily get absorption coefficient α by:

$$\alpha = \frac{\sqrt{2}\omega}{c} \sqrt{|\varepsilon(\omega)| - \text{Re}\varepsilon(\omega)}. \quad (3)$$

The method to calculate these optical parameters is fully explained in Ref. 38.

The absorption spectrum for pure graphene and B, N, O and F doped graphene for both cases of in plane polarization of light ($E \perp c$) and out of plane polarization of light ($E \parallel c$), are shown in Figs. 3(a)-(b). The energy interval was set from 0 to 25 eV for calculating the absorption coefficient.

First, we calculated the absorption coefficient of pure graphene. Our result shows that pure graphene absorption spectrum for in-plane polarization of light ($E \perp c$) has two main peaks at 4.3 eV and 14.2 eV with an intensity of approximately 4000 cm^{-1} and $95,000 \text{ cm}^{-1}$, respectively and has zero absorption in the interval from 7 to 11 eV. The first main peak arises from the transition from $\pi \rightarrow \pi^*$ and second from $\sigma \rightarrow \sigma^*$, which is shown in the density of state diagram, Fig. 3(a), by the arrows A and B, respectively. For out of plane polarization of light ($E \parallel c$) on graphene layer in the energy region from 0 to 10 eV, absorption is zero and two sharp peaks locate at 11.6 eV and 14.67 eV with intensity of approximately $62,800 \text{ cm}^{-1}$ and $66,400 \text{ cm}^{-1}$. These results are in agreement with the other reports [39]. In this case, the first peak arises from $\pi \rightarrow \sigma^*$ transition and second from $\sigma \rightarrow \pi^*$ transition, which is shown in Fig. 3(b) by the arrows C and D, respectively.

For in-plane polarization of light ($E \perp c$) as can be seen from Fig. 3(a), for graphene doped with various atoms, all absorption peaks have shifted toward larger energies (blue shift). These displacements for the 4.3 eV peak are larger than 14.2 eV peak; it can be concluded that the graphene doped by different atoms is more affected in absorption value at lower energy. In graphene doped with various atoms and graphene with a vacancy, as seen from DOS diagrams, Figs. 4(b)–(f), the states near Fermi level are more affected, as a result, the absorption spectrum undergoes further changes in lower energy that can be seen from Fig. 3(a). In other

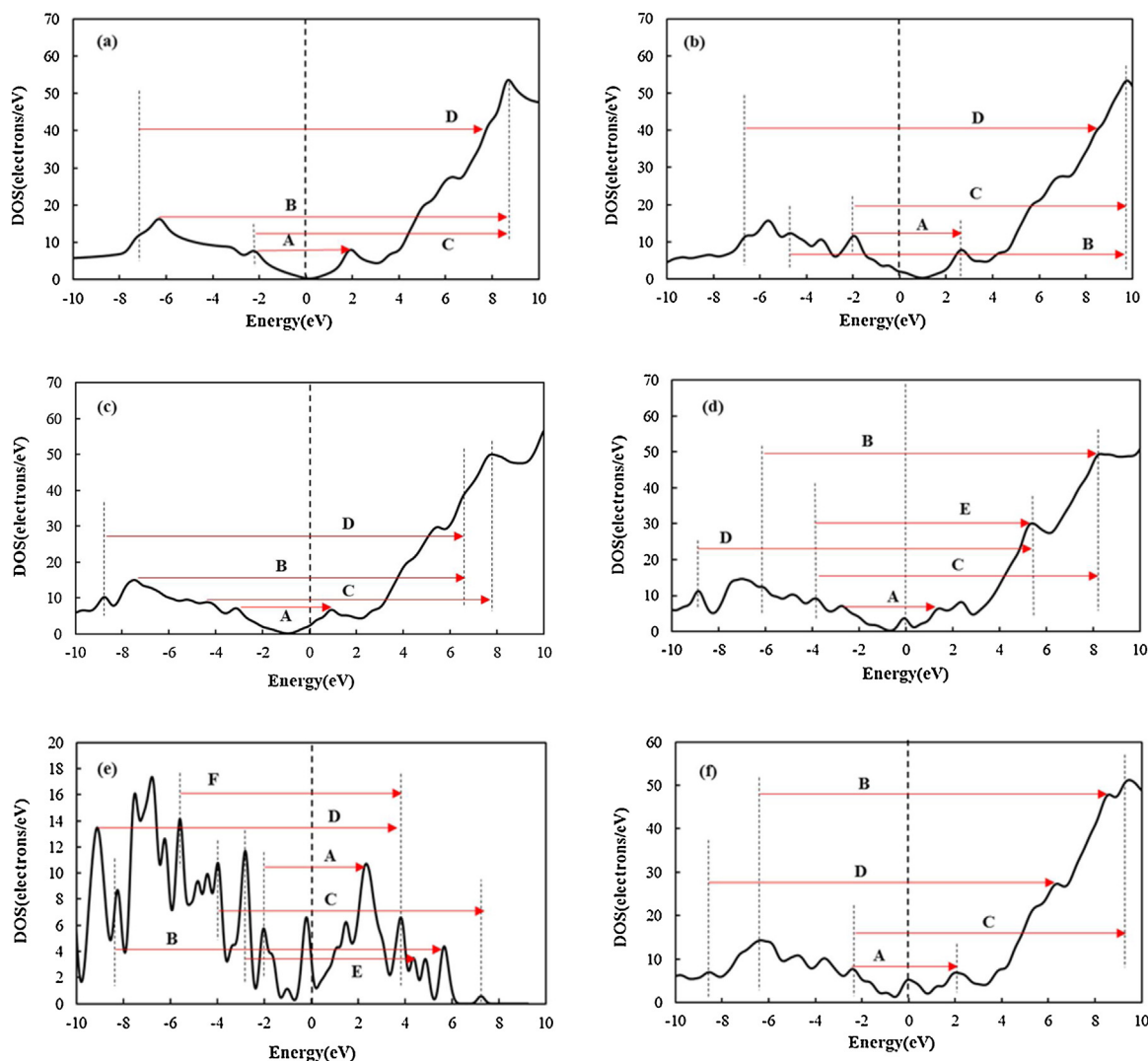


Fig. 4. DOS of (a) pure graphene in the 4×4 supercell, (b) B doped graphene, (c) N doped graphene, (d) O doped graphene, (e) F doped graphene and (f) graphene with a vacancy.

words doping in graphene with various atoms is more effective in π and π^* bands displacement than σ and σ^* bands. As seen from Fig. 3(a) graphene has adsorption for low energy (about 2 eV) which represents its metallic property. By doping graphene with different atoms, this absorption peak clearly moves to more energy like as two main peaks.

In the case of B and N doped graphenes, the two main peak shifts are negligible because band gap is very small, and only Fermi level shifts that is consistent with previous work [40]. As already mentioned, in the range from 7 to 11 eV energies, absorption spectra for pure graphene is zero like for B and N doped graphene.

For O and F doped graphene, both main peaks clearly have been shifted to the larger energies, although the first peak displacement is larger than the second peak, which is in more energy. This change in near states to Fermi level is due to the addition of O and F atom to pure graphene. As shown in Fig. 3(a), for O doped graphene in the range from 7 to 11 eV energy, a clear peak is seen and for F doped graphene two weak peaks are seen. By looking at density of state diagram near Fermi level between the valence and conduction bonds, there are additional states whose origin is s and p orbital hybridization of O and F atoms with the s and p orbitals nearest carbon atoms in the graphene layer and this causes to create an additional peak in the range from 2 to 7 eV in absorption spectrum

for O doped graphene and increasing the number of peaks in this energy range to two peaks is due to separation of spin up and down levels for F doped graphene. The electron excitations that cause these peaks in the absorption spectra are represented by arrows E and F in the O and F doped graphene DOS diagram, Fig. 4(d) and (e).

For graphene with a vacancy as in the case of B and N doped graphene, the main absorption peaks (at 4.3 eV and 14.2 eV) have been moved very little to larger energies and there is no additional peak between the two main peaks. The intensity of all absorption peaks in the presence of one of the impurity atoms is less than peak intensity in pure graphene, and peak absorption intensities for O and F doped graphene are less than B and N doped graphene. In case of graphene with the vacancy as can be seen in Fig. 4(f) the high of the peak in 4.3 eV, is more than this peak for pure graphene. According to the golden rule of Fermi reducing the absorption peak intensity in doped graphene structures is due to the decrease in the density of state peaks that are connected with the arrows to illustrate the excitations.

Absorption spectra of doped graphene layers for $(E \parallel c)$, Fig. 3(b), in all cases absorption is zero for the energy region from 0 to 10 eV, like as pure graphene and two main absorption peaks move toward larger energies (blue shift), but graphene with a vacancy, B and N doped graphene has lower absorption peak shifts compared to O

and F doped graphene as in the case that field is parallel to the graphene layer. In all structures intensity of these peaks is less than pure graphene. Optical absorption of pure graphene, graphene with a vacancy and doped graphene due to the anisotropy of the charge distribution of inside and outside layer is anisotropic for in plane and out of plane light polarization.

Conclusions

In this work DFT was employed to calculate the structural and optical properties of graphene with a vacancy and B, N, O and F doped graphene. We found that B doped graphene is a p-type semiconductor and the other structure are n-type. Band gap of B, N and O graphene doped structures respectively are equal to 0.186 eV, 0.203 eV and 0.494 eV and for F doped graphene this value is different for the spin up and down equal to 0.367 eV and 0.546 eV, respectively, therefore the recent structure is noteworthy for spintronic tool design. Furthermore, absorption spectrum has been calculated for light polarization parallel and perpendicular to the plane of the graphene layer and the results show that all absorption peaks have shifted toward larger energies (blue shift) and peak intensities decrease with increasing number of electrons entering the structure.

Author contribution statement

- this material has not been published in whole or in part elsewhere;
- the manuscript is not currently being considered for publication in another journal;
- all authors have been personally and actively involved in substantive work leading to the manuscript, and will hold themselves jointly and individually responsible for its content;
- In the calculations, the non-commercial Quantum Espresso code has been used;
- Dr. S.S. Parhizgar conceived of the presented idea. M. Goudarzi developed the theory and performed the computations. Dr. S.S. Parhizgar and Dr. J. Beheshtian verified the analytical methods and encouraged M. Goudarzi to investigate [a specific aspect] and supervised the findings of this work. All authors discussed the results and contributed to the final manuscript.

References

- [1] K.S. Novoselov, A.K. Geim, S. Morozov, D. Jiang, Y. Zhang, S.V. Dubonos, I.V. Grigorieva, A.A. Firsov, Electric field effect in atomically thin carbon films, *Science* 306 (2004) 666–669, <http://dx.doi.org/10.1126/science.1102896>.
- [2] K.S. Novoselov, A.K. Geim, S. Morozov, D. Jiang, M.I. Katsnelson, I.V. Grigorieva, S.V. Dubonos, A.A. Firsov, Two-dimensional gas of massless Dirac fermions in graphene, *Nature (London)* 438 (2005) 197–200, <http://dx.doi.org/10.1038/nature04233>.
- [3] C. Meyer Jannik, A.K. Geim, M.I. Katsnelson, K.S. Novoselov, T.J. Booth, S. Roth, The structure of suspended graphene sheets, *Nature (London)* 446 (2007) 60–63, <http://dx.doi.org/10.1038/nature05545>.
- [4] T. Eberlein, U. Bangert, R.R. Nair, R. Jones, M. Gass, A.L. Bleloch, K.S. Novoselov, A. Geim, P.R. Briddon, Plasmon spectroscopy of free-standing graphene films, *Phys. Rev. B* 77 (2008) 233406, <http://dx.doi.org/10.1103/PhysRevB.77.233406>.
- [5] J.L. Cheng, C. Salazar, J.E. Sipe, Optical properties of functionalized graphene, *Phys. Rev. B* 88 (2013) 045438, <http://dx.doi.org/10.1103/PhysRevB.88.045438>.
- [6] F. Bonaccorso, Z. Sun, T. Hasan, A.C. Ferrari, Graphene photonics and optoelectronics, *Nat. Photonics* 4 (2010) 611–622, <http://dx.doi.org/10.1038/nphoton.2010.186>.
- [7] L. Liu, H. Yao, H. Li, Z. Wang, Y. Shi, Recent advances of low-dimensional materials in lasing applications, *FlatChem* 10 (2018) 22–38, <http://dx.doi.org/10.1016/j.flatc.2018.09.001>.
- [8] S. Kumari, H.P. Mungse, R. Gusain, N. Kumar, H. Sugimura, O.P. Khatri, Octadecanethiol-grafted molybdenum disulfide nanosheets as oil-dispersible additive for reduction of friction and wear, *FlatChem* 3 (2017) 16–25, <http://dx.doi.org/10.1016/j.flatc.2017.06.004>.
- [9] X. Wang, L. Zhi, K. Mullen, Transparent, conductive graphene electrodes for dye-sensitized solar cells, *Nano Lett.* 8 (2008) 3233–3237, <http://dx.doi.org/10.1021/nl072838r>.
- [10] W.H. Liu, T. Dang, Z.H. Xiao, X. Li, C. Zhu, X. Wang, Carbon nanosheets with catalyst-induced wrinkles formed by plasma-enhanced chemical-vapor deposition, *Carbon* 49 (2011) 884–889, <http://dx.doi.org/10.1016/j.carbon.2010.10.049>.
- [11] M.D. Stoller, S. Park, Y. Zhu, J. An, R.S. Ruoff, Graphene-based ultracapacitors, *Nano Lett.* 8 (2008) 3498–3502, <http://dx.doi.org/10.1021/nl802558y>.
- [12] O.V. Yazyev, M.I. Katsnelson, Magnetic correlations at graphene edges: basis for novel spintronics devices, *Phys. Rev. Lett.* 100 (2008) 047209, <http://dx.doi.org/10.1103/PhysRevLett.100.047209>.
- [13] O.V. Sedelnikova, L.G. Bulusheva, A.V. Okotrub, Ab initio study of dielectric response of rippled graphene, *J. Chem. Phys.* 134 (2011) 244707, <http://dx.doi.org/10.1063/1.3604818>.
- [14] K.M. McCreary, K. Pi, A.G. Swartz, W. Han, W. Bao, C.N. Lau, F. Guinea, M.I. Katsnelson, R.K. Kawakami, Effect of cluster formation on graphene mobility, *Phys. Rev. B* 81 (2010) 115453, <http://dx.doi.org/10.1103/PhysRevB.81.115453>.
- [15] C.P. Herrero, R. Ramirez, Diffusion of hydrogen in graphite: a molecular dynamics simulation, *J. Phys. D* 43 (2010) 255402, <http://dx.doi.org/10.1088/0022-3727/43/25/255402>.
- [16] E.J. Doppluck, M. Scheffler, Ph.D. Lindan, Hallmark of perfect graphene, *J. Phys. Rev. Lett.* 92 (2004) 22, <http://dx.doi.org/10.1103/PhysRevLett.92.225502>.
- [17] K. Pi, K.M. McCreary, W. Bao, W. Han, Y.F. Chiang, Y. Li, S.W. Tsai, C.N. Lau, R.K. Kawakami, Electronic doping and scattering by transition metals on graphene, *Phys. Rev. B* 80 (2009) 075406, <http://dx.doi.org/10.1103/PhysRevB.80.075406>.
- [18] P.A. Denis, Band gap opening of monolayer and bilayer graphene doped with aluminium, silicon, phosphorus, and sulfur, *Chem. Phys. Lett.* 492 (2010) 251–257, <http://dx.doi.org/10.1016/j.cplett.2010.04.038>.
- [19] M. Rafique, Y. Shuai, H.P. Tan, M. Hassan, Structural, electronic and magnetic properties of 3d metal trioxide clusters-doped monolayer graphene: a first-principles study, *Appl. Surface Science* 399 (2017) 20–31, <http://dx.doi.org/10.1016/j.apsusc.2016.12.017>.
- [20] M.S. Sharif Azadeh, A. Kokabi, M. Hosseini, M. Fardmanesh, Tunable bandgap opening in the proposed structure of Nitrogen-doped graphene, *Micro & Nano Lett.* 6 (8) (2011) 582–585, <http://dx.doi.org/10.1049/mnl.2011.0195>.
- [21] Y.H. Ho, J.Y. Wu, Y.H. Chiu, J. Wang, M.F. Lin, Electronic and optical properties of monolayer and bilayer graphene, *Philos. Trans. Math. Phys. Eng. Sci.* 368 (2010) 5445–5458, <http://dx.doi.org/10.1098/rsta.2010.0209>.
- [22] M. Wu, C. Cao, J.Z. Jiang, Light non-metallic atom (B, N, O and F)-doped graphene: a first-principles study, *Nanotechnology*, 21 (2010) 505202, <http://dx.doi.org/10.1088/0957-4484/21/50/505202>.
- [23] P. Giannizzi, S. Baroni, N. Bonini, M. Calandra, R. Car, C. Cavazzoni, D. Ceresoli, G.L. Chiarotti, M. Cococcioni, I. Dabo, A. Dal Corso, S. de Gironcoli, S. Fabris, G. Fratesi, R. Gebauer, U. Gerstmann, C. Gougousis, A. Kokalj, M. Lazzeri, L. Martin-Samos, N. Marzari, F. Mauri, R. Mazzarello, S. Paolini, A. Pasquarello, L. Paulatto, C. Sbraccia, S. Scandolo, G. Scalapuzo, A.P. Seitsonen, A. Smogunov, P. Umari, R.M. Wentzcovitch, QUANTUM ESPRESSO: a modular and open-source software project for quantum simulations of materials, *J. Phys. Condens. Matter* 21 (2009) 395502, <http://dx.doi.org/10.1088/0953-8984/21/39/395502>.
- [24] J.P. Perdew, K. Burke, M. Ernzerhof, Generalized gradient approximation made simple, *Ann. Readapt. Med. Phys.* 77 (1996) 3865, <http://dx.doi.org/10.1103/PhysRevLett.77.3865>.
- [25] Y. Wang, Y.Y. Shao, D.W. Matson, J.H. Li, Y.H. Lin, Nitrogen-doped graphene and its application in electrochemical biosensing, *ACS Nano* 4 (2010) 1790–1798, <http://dx.doi.org/10.1021/nn100315s>.
- [26] X. Zheng, J. Zhicheng, Z. Yulong, W. Jialu, Z. Yabo, Q. Yinghui, Q. Yitai, One-pot hydrothermal synthesis of Nitrogen-doped graphene as high-performance anode materials for lithium ion batteries, *Science Report* 6 (2016) 26146, <http://dx.doi.org/10.1038/srep26146>.
- [27] R. Satio, G. Dresselhaus, M.S. Dresselhaus, *Physical Properties of Carbon Nanotubes*, Imperial College, London, 1998.
- [28] J.P. Perdew, Y. Wang, Accurate and simple analytic representation of the electron-gas correlation energy, *Phys. Rev. B* 45 (1992) 13244, <http://dx.doi.org/10.1103/PhysRevB.45.13244>.
- [29] S. Agnoli, M. Favaro, Doping graphene with boron: a review of synthesis methods, physicochemical characterization, and emerging applications, *J. Mater. Chem. A Mater. Energy Sustain.* 4 (2016) 5002–5025, <http://dx.doi.org/10.1039/C5TA10599D>.
- [30] L.S. Panchakarla, K.S. Subrahmanyam, S.K. Saha, A. Govindaraj, H.R. Krishnamurthy, U.V. Waghmare, C.N.R. Rao, Synthesis, Structure and Properties of Boron and Nitrogen Doped Graphene, *Condens. Matter Phys.* 21 (2009) 4726–4730, <http://dx.doi.org/10.1002/adma.200901285>.
- [31] X. Wang, X. Li, L. Zhang, Y. Yoon, P.K. Weber, H. Wang, N-doping of graphene through electrothermal reactions with Ammonia, *Science* 324 (2009) 768–771, <http://dx.doi.org/10.1126/science.1170335>.
- [32] M. Rafique, Y. Shuai, H.P. Tan, M. Hassan, Manipulating intrinsic behaviors of graphene by substituting alkaline earth metal atoms in its structure, *RSC Adv.* 7 (2017) 16360–16370, <http://dx.doi.org/10.1039/C7RA01406F>.
- [33] M. Rafique, Y. Shuai, H.P. Tan, First-principles study on hydrogen adsorption on nitrogen doped graphene, *Low Dimens. Syst. Nanostruct.* 88 (2017) 115–124, <http://dx.doi.org/10.1016/j.physe.2016.12.012>.

- [34] F. banhart, J. Kotakoski, A.V. krashennnikov, Structural defect in graphene, *ACS Nano* 5 (1) (2011) 26–41, <http://dx.doi.org/10.1021/nn102598m>.
- [35] R.I. Masel, *Principles of Adsorption and Reaction on Solid Surfaces*, John Wiley and Sons, New York, 1996.
- [36] S.S. Zumdahl, *Chemical Principles*, fifth ed., Mifflin Company, Houghton, 2005.
- [37] Z. Ao, S. Li, hydrogenation of graphene and hydrogen diffusion behavior on graphene/Graphane interfac, in: J.R. Gong (Ed.), *Graphene Simulation*, InTech, Croatia, 2011, 53-74.
- [38] A. Marinopoulos, L. Reining, A. Rubio, V. Olevano, Ab initio study of the optical absorption and wave-vector-dependent dielectric response of graphite, *Condens. Matter Phys.* 69 (2004) 245419, <http://dx.doi.org/10.1103/PhysRevB.69.245419>.
- [39] Z. Sun, Z. Yan, J. Yao, E. Beitler, Y. Zhu, J.M. Tour, Growth of graphene from solid carbon sources, *Nature* 468 (2010) 549–552, <http://dx.doi.org/10.1038/nature09579>.
- [40] P. Rani, G.S. Dubey, V.K. Jindal, DFT study of optical properties of pure and doped Graphene, *Physica. E. Low. Syst. Nanostruct.* 62 (2014) 28–35, <http://dx.doi.org/10.1016/j.physe.2014.04.010>.